Journal of the European Ceramic Society 21 (2001) 2149–2151

www.elsevier.com/locate/jeurceramsoc

Image analysis of multiphased ceramics

P. Belhomme, D. Houivet, W. Lecluse, J.M. Haussonne *

Laboratoire Universitaire des Sciences Appliquées de Cherbourg, Université de Caen Basse Normandie, LUSAC, Site Universitaire de Cherbourg, BP 78, 50130 Octeville, France

Received 4 September 2000; received in revised form 20 November 2000; accepted 5 December 2000

Abstract

In this study, we focus on the recognition and characterization of the different phases present in a $(Zr,Sn)TiO_4$ ceramic (with some amounts of La_2O_3 and NiO as sintering aids). Our work deals with the study of segmentation techniques that automatically extract each of the phases (ZST, TiO_2, $La_{2/3}TiO_3$,...) from a scanning electronic microscope image of a polished section of the ceramic. The main difficulty encountered at this stage of the work is that their properties in terms of gray levels are very close together, thus, imposing the combination of simple image processing operators (such as thresholding) with advanced methods based on region growing processes.

Keywords: Electron microscopy; Image processing; Microstructure-final

1. Introduction

The microwave characteristics of $(Zr,Sn)TiO_4$ dielectric ceramics for filters or resonators are highly dependent on the process. More precisely, these ceramics are multiphased, the nature, amount and shape of the different phases depending on the whole steps of the ceramic process.[1] So, it is important to be able to evaluate and quantify in an automatic way the influence of the different process parameters on the size of the ceramic grains, on the amount and repartition of the different secondary phases, etc. It is typically in this kind of situation that image processing appears to be an interesting tool, thanks to the great performances available with PCs.

2. Materials

SEM micrographs of ceramics from the composition diagram ZrO_2–SnO_2–TiO_2 (with some amounts of La_2O_3 and NiO as sintering aids) were acquired at 500 magnification with a secondary electrons detector (acceleration voltage: 20 kV, working distance: 25 mm). Ceramics have previously been polished and sputtered with gold.

The image size is 512×368, each pixel being coded by one byte (256 gray levels possible). Fig. 1 shows a typical image to be processed, which was obtained after a smoothing step by a gaussian filter (size 3, $\sigma = 5$) for reducing acquisition noise.

Considering the gray level distribution (see histogram Fig. 2), the operator has to center the ZST peak on the value 128, then to tune acquisition devices in order to spread out the image gray levels on the whole available range. A slight saturation is thus encountered for hole side reflections. In the presented example five classes have to be extracted, which are respectively:

- in black: holes;
- in dark gray: TiO_2 phase;
- in gray: ZST phase (corresponding to the image background);
- in light gray: $La_{2/3}TiO_3$ phase;
- in white: hole side reflections.

In this work, we have used two image processing softwares. The first one is a commercial toolbox based on a graphical user interface (GUI) for rapid testing of the operators to be used. The other one, developed in a laboratory of our University, allows the creation of an executable file leading to the complete automation of

* Corresponding author. Tel.: +33-02-3301-4214; fax: +33-02-3301-4201.

E-mail address: jmhaussonne.lusac@chbg.unicaen.fr (J.M. Haussonne).

0955-2219/01/$ - see front matter
PII: S0955-2219(01)00191-1

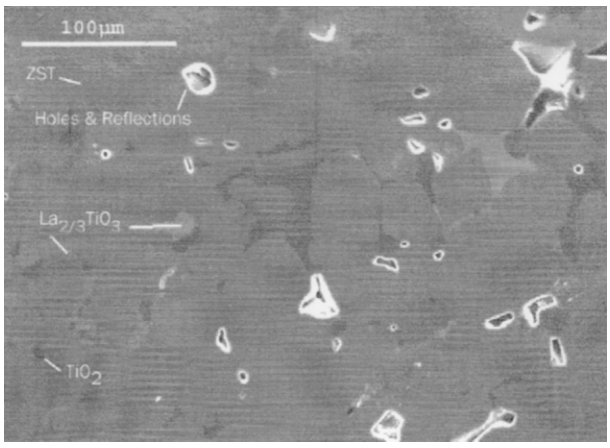

Fig. 1. Example of ceramic microstructure to be analyzed (*Im*1).

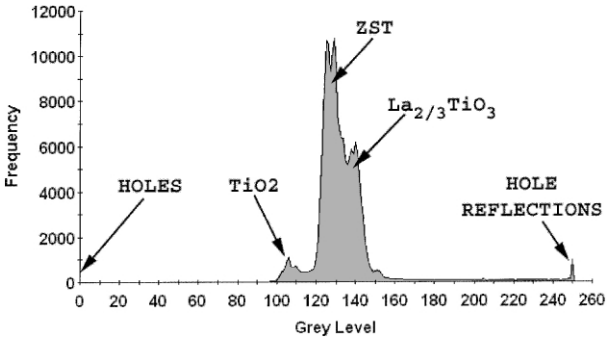

Fig. 2. Gray level histogram of *Im*1 with the five classes.

the analysis. The first software is APHÉLION© (ADCIS, 10 avenue de Garbsen, 14200 Hérouville St Clair, France), the second one is PANDORE (GREYC Laboratory, UPRESA CNRS 6072, Bd Maréchal Juin, 14072 Caen Cedex, France).

3. Methods

The gray-level distribution of this image type presents some particular and reproducible characteristics according to ceramic phases. Some of these phases are associated with isolated peaks in the histogram (holes and reflections, TiO_2) and can, therefore, be well segmented thanks to simple thresholding. Some other phases show overlapping peaks that can no longer be separated by thresholding (in this example ZST and TiLa). Region-based image processing methods thus appear as a good solution combining performance and simplicity. Automatic segmentation of ceramic phases may then be achieved in three steps:

- extraction of black holes and their associated white reflections by thresholding,
- extraction of TiO_2 phase also by thresholding,
- splitting of ZST and TiLa phases by a region growing method under constrained markers.

3.1. Hole and reflection extraction

Since the acquisition parameters are tuned in order to have a ZST peak centered in the gray-level histogram, the original smoothed image (so-called *Im*1) is arbitrarily held in the threshold between 0 and 128. The obtained binary mask (so-called *Msk-inf*) is applied onto *Im*1 to keep the lowest gray-levels. These pixels are then split in three classes by Fisher's "thresholding" algorithm based on a minimization of intra-class variances.[2,3] It allows extracting black holes in ceramics, which correspond to the first class returned by the algorithm (so-called *Msk-BlackHoles*).

The inverse binary mask of *Msk-inf* is applied onto *Im*1 to keep the highest gray levels. The same splitting process is done again, this time with 4 classes, in order to extract pixels belonging to reflections encountered at the border of black holes. These pixels are in the two last classes returned by Fisher's algorithm (so-called *Msk-Reflections*).

A logical "OR" between *Msk-BlackHoles* and *Msk-Reflections*, followed by a morphological closing of size 2 and a filling step achieved with the "Hole filling" morphological operator[4] allows one to obtain a binary mask of holes and their associated reflections in ceramics (see Fig. 3). The inverse binary mask applied onto *Im*1 enables to separate pixels corresponding to the remaining ZST, TiO_2 and $La_{2/3}TiO_3$ phases. The next image processing steps will then be performed onto this reduced gray-level image (so-called *Im*2).

3.2. TiO_2 extraction

The central part of the histogram in Fig. 2 shows that the TiO_2 phase is clearly dissociated from the ZST phase by a valley. Here again, Fisher's algorithm can be used to split the two peaks. Considering the shape of the central part, the automatic splitting has to be achieved with four classes, TiO_2 pixels thus belonging to the first one (see the corresponding TiO_2 binary mask in Fig. 4). The inverse TiO_2 binary mask applied onto *Im*2 isolates

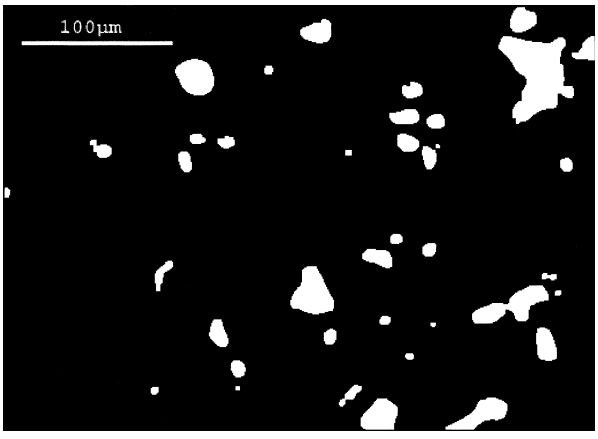

Fig. 3. Binary mask after the hole extraction (holes + reflections).

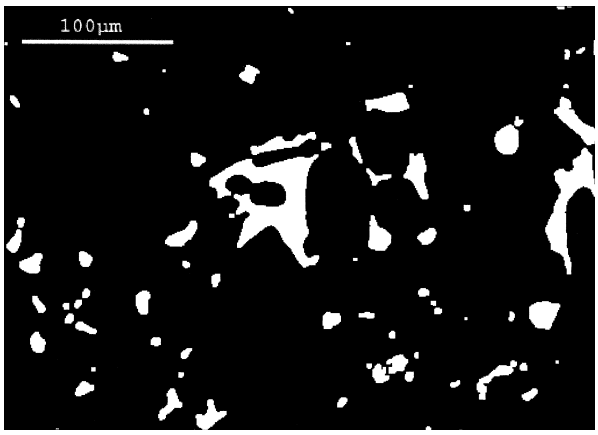

Fig. 4. Binary mask of the TiO_2 phase.

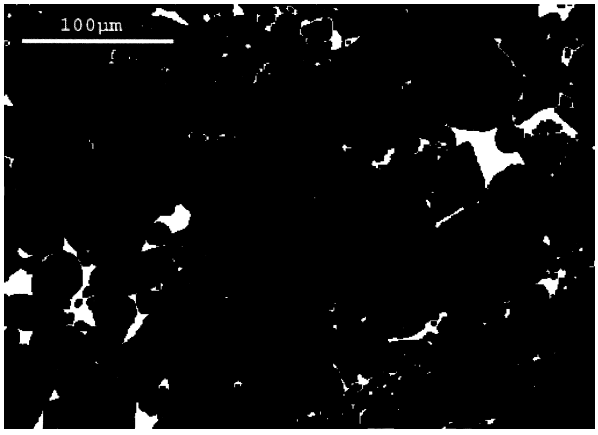

Fig. 5. Binary mask of the $La_{2/3}TiO_3$ phase.

pixels corresponding to the sole ZST and $La_{2/3}TiO_3$ phases, giving a new gray-level image so-called *Im*3.

3.3. ZST and $La_{2/3}TiO_3$ splitting

Splitting of these two phases is a more difficult operation, as there is a strong mixing of their peaks in the gray-level histogram. In this case, any thresholding method can no longer provide a good result. The idea is then to attempt to extract regions of connected pixels for which gray-level values are very close.[5,6] So, an image of seeds exactly located in the ZST phase has first to be computed, the best way being to consider pixels with the lowest gray values in *Im*3. Then, a region growing process is achieved by merging pixels in the neighborhood of seeds when the difference between their gray-level value and the mean value of the adjacent region is lower than a given parameter (empirically tested and set to 5 gray-levels/256 possible in our application). Once this step is completed, all pixels of the ZST phase are extracted to form a binary mask. Its complementary thus contains the $La_{2/3}TiO_3$ phase (see Fig. 5).

4. Results

One main piece of information that can be obtained by automatic analysis of ceramic images is the area density of the different phases present. It is noteworthy that the calculated data correspond to the ratio of the number of pixels belonging to a given phase by the total number of pixels of the image (512×368 in the present example). So, the accuracy of these results is infinite and must not be confused with the error of measurement associated with the evaluation of the different present phase's amounts. It is also noteworthy that, if the ceramic process, as it is generally the case, yields to isotropic materials and if the analyzed areas are randomly chosen, the stereology theories demonstrate that the area density is equivalent to the volume density.[7]

For the present example, we finally get the following area densities:

Holes and reflections:	6.5%	$La_{2/3}TiO_3$:	3.7%
TiO_2:	7.7%	ZST:	82.1%

5. Discussion

This study shows that it is possible to automatically extract relevant information such as area density. It is also possible to compute size distribution or shape factors of phases present in ceramics. Nevertheless, the gray-level distributions of images to be processed have to be well analyzed in order to choose and adapt available segmentation operators. Practically, a combination of "thresholding" methods and region-based methods provides the best compromise between performance and simplicity.

References

1. Houivet, D., El Fallah, J. and Haussonne, J. M., Phases in La_2O_3 and NiO doped (Zr,Sn)TiO_4 microwave dielectric ceramics. *J. Eur. Ceram. Soc.*, 1999, **19**, 1095–1099.
2. Fisher, W. D., On grouping for maximum homogeneity. *JASA*, 1958, **53**, 789–798.
3. Sahoo, P. K., Soltani, S., Wong, A. K. C. and Chen, Y. C., A survey of thresholding techniques. *CVGIP*, 1988, **41**, 233–260.
4. Serra, J., *Image Analysis and Mathematical Morphology: Theoretical Advances, Vol. 2*. Academic Press, London, 1988.
5. Clermont, P. and Cartier, S., Implementation and evaluation of region growing algorithms on CM2. In *Proceedings of the Int. Colloquium on Parallel Image Processing*, Paris, 1991, pp. 91–109.
6. Cocquerez, J. P. and Philipp, S., *Analyse d'Images: Filtrage et Segmentation*. Ouvrage coll. GdR 134, Masson, Paris, 1995.
7. Cruz-Orive, L. M., Stereology of single objects. *Journal of Microscopy*, 1997, **186**(2), 93–107.